



*Research Article / Araştırma Makalesi*

## **Aerodynamic performance comparison of circular and rectangular S-ducts for aircraft intakes: A CFD study/ Uçak hava alğı için dairesel ve dikdörtgen S-kanallarının aerodinamik performans karşılaştırması: Bir CFD çalışması**

 Mehmet Turan Ekinci<sup>1\*</sup>,  Mahmut Sami Bük<sup>2</sup>

<sup>1</sup>Aerospace Engineering, Faculty of Engineering, OSTİM Technical University, Ankara, Türkiye

<sup>2</sup>Aeronautical Engineering, Faculty of Aeronautics and Astronautics, Necmettin Erbakan University, Konya, Türkiye

**Received**  
February 10, 2025

**Revised**  
May 13, 2025

**Accepted**  
May 15, 2025

### **Keywords**

*Aerodynamic performance,  
Computational fluid  
dynamics,  
Efficiency,  
S-ducts*

### **Anahtar Kelimeler**

*Aerodinamik performans,  
Hesaplamalı akışkanlar  
dinamiği,  
S-kanal,  
Verimlilik*

Production and hosting by  
[Turkish DergiPark](https://dergipark.org.tr/en/pub/ijaa). This is  
an open access article  
under the CC BY-NC  
license  
(<https://creativecommons.org/licenses/by-nc/4.0/>).



### **ABSTRACT**

S-ducts are critical engine inlet components designed to optimize aerodynamics and flight performance, enhance efficiency, and ensure smooth airflow in both aerospace and automotive applications. These ducts are used to direct and deliver airflow to the engine, improving engine performance, increasing fuel efficiency, and minimizing effects such as turbulence. In military jets, S-ducts also serve as structures that enhance maneuverability and absorb incoming radar waves. Additionally, by smoothing the airflow, S-ducts play a significant role in noise reduction. However, secondary flows and flow separation can sometimes occur within S-ducts. These phenomena may negatively impact the performance of S-ducts, leading to a reduction in overall flight performance.

In this study, 3D models of circular and rectangular S-ducts were created using SOLIDWORKS to observe variations in velocity, pressure, flow distribution, and kinetic energy within ducts of different geometries. Flow analysis was carried out using the SST  $k-\omega$  turbulence model in ANSYS Fluent. The analysis produced results for pressure, velocity, and kinetic energy. The findings indicated that although the pressure and velocity distributions were more uniform in the rectangular S-duct, the circular S-duct showed better performance in terms of pressure recovery and distortion coefficient.

### **ÖZET**

S-kanallar, aerodinamik ve uçuş performansını optimize etmek, verimliliği artırmak ve hem havacılık hem de otomotiv uygulamalarında düzgün hava akışı sağlamak için tasarlanmış önemli motor giriş kanallarıdır. Bu kanallar, hava akışını motora yönlendirmek ve iletmek, motor performansını iyileştirmek, yakıt verimliliğini artırmak ve türbülans gibi etkileri en aza indirmek için kullanılır. Askeri jetlerde, S-kanallar manevra kabiliyetini artıran ve gelen radar dalgalarını emebilen yapılardır. Ek olarak, S-kanallar hava akışını yumuşatarak gürültüyü azaltma da önemli bir rol oynar. S-kanallarda bazen ikincil akışlar ve akış ayrımı meydana gelebilir. İkincil akışlar ve akış ayrımı, S-kanallardaki performans üzerinde olumsuz bir etkiye sahip olabilir ve bu da uçuş performansında düşüşe yol açabilir.



Bu çalışmada, farklı geometriye sahip kanal içindeki hız, basınç, akış dağılımı ve kinetik enerji değişimlerini gözlemlemek için SOLIDWORKS kullanılarak dairesel ve dikdörtgen S-kanallar için 3B modeller oluşturuldu. Akış analizi, SST k- $\omega$  türbülans modeli uygulanarak ANSYS Fluent programıyla gerçekleştirildi. Analizlerde basınç, hız ve kinetik enerji için sonuçlar elde edildi. Bulgular, dikdörtgen S-kanalda basınç ve hız dağılımı daha düzgün olmasına rağmen, dairesel S-kanalının basınç geri kazanımı ve bozulma katsayısı açısından dikdörtgen S-kanaldan daha iyi sonuçlar verdiğini göstermiştir.

\* Corresponding author, e-mail: [mehmet.ekinci@ostimtekniik.edu.tr](mailto:mehmet.ekinci@ostimtekniik.edu.tr)

## 1. Introduction

Multiple factors such as high pressure recovery, low drag value, low radar visibility and noise level, and minimum weight should be taken into consideration in aircraft intake design [1]. The main reason for using this component in combat aircrafts is to reduce the radar cross-section. However, designing and configuring it to achieve this reduction is a complex process [1]. Some aircraft feature an S-duct, an essential propulsion system component with an S-shaped curve to direct airflow to the engine, commonly used in military aircraft like the F-22 Raptor and certain civilian models [2]. It is important to ensure that the aircraft engine is properly supplied with air under all flight conditions [3]. Additionally, optimum design of S-ducts requires ensuring and controlling the flow pattern in the ducts [4]. S-ducts have also been used as a solution for positioning the central engine in tri-engine aircraft, and most tri-engine aircraft designs favor the use of S-ducts [5]. This structure, which has rectangular and circular inlet cross-sections, can have different turning angles and curvatures in the duct [5]. Due to the curvature in the S-duct design, issues such as pressure gradients, secondary flows and flow separation that can affect flight performance may occur [6]. As a key component in embedded propulsion systems, the S-duct presents particular challenges. Flow separation within the S-duct occurs due to the curvature of the centerline and the diffusion geometry, causing distortions and significant disruptions to the airflow [7]. As this crucial element has substantial impacts on aircraft's performance, there are many S-duct studies in the existing literature proposed by various researchers. To name a few;

Rk et al. [5] performed CFD (Computational Fluid Dynamics) analyses for 3 different S-duct designs with rectangular, circular and elliptical cross-sectional areas and proved that the duct with elliptical cross-sectional area yields better results in automobile and other vehicle applications.

Papadopoulos et al. [8] design a CAD (Computer Aided Design) model of a S-duct to specify optimal parameters for UAV (Unmanned Aerial Vehicle) application. In the study, the Gerlach shaped design was adopted to reduce the strength of secondary vortices and was proved that it was a good choice. The study also shows that the axial length should be changed to find the optimum length according to the total pressure losses. To carry out that a commercial flow solver program was used for flow field calculation. It was explained that the design should be tested experimentally to verify the findings of the analyses performed.

Thenambika et al. [3] performed CFD analysis for S-duct with submerged vortex generators and normal S-duct at 0.6 Mach and 1.0 Mach. It was found that the static pressure recovery would increase as the flow moved on along the duct, except at the beginning of the S-duct. As a result of the analysis of S-duct and S-duct with submerged vortex generators at 0.6 and 1 Mach numbers, it was concluded that the best result was obtained at 0.6 Mach number.

Saha et al. [9] studied the effects of ducts with different cross-sectional shapes for intake using the k- $\epsilon$  turbulence model and found that the elliptically shaped inlet had the best results, while the squared shaped inlet had the worst results in pressure recovery, loss coefficient, and flow distortion at the engine face.



Migliorini et al. [10] represents an important step in characterizing the time-dependent disturbance under various inlet conditions, unlike previous studies. The research evaluated the effect of the thickness and orientation of the inlet vortices and the inlet total pressure profiles at different strengths and locations. As a result, it is suggested to evaluate the flow disturbance characteristics of S-ducts not only under uniform inlet conditions but also under different inlet conditions.

Xiao et al. [11] applied the lagged  $k-\omega$  model to investigate the flow characteristics of the diffuser in a transonic flow. The study shows that the  $k-\omega$  turbulence model with the addition of a lag model performs better in regions where flow separation occurs. The objectives of the study are to model turbulent flows with strong shock wave-boundary layer interactions more accurately and to demonstrate that a significant improvement is achieved when the lag model is used.

Zhang et al. [12] conducted a design study using the Shear Stress Transport (SST)  $k-\omega$  turbulence model for analysis. In the paper, a modified SST turbulence model is proposed and validated. The study demonstrates the advantages of using a modified turbulence model and automatic optimization system to improve the S-duct design process. In addition, while aerodynamic performance is increased at low velocity, high velocity performance is decreased.

McLelland et al. [13] carried out a detailed experimental study to determine the effect of the intake flow profile on the intake flow disturbance at the outlet of the S-duct inlet. The thickness of the boundary layer and appropriate levels of asymmetry should be considered to ensure that the temporal and spatial characteristics of the inlet flow are accurately represented.

Aslan [15] investigated the pressure losses and distortions along the aerodynamic interface plane and obtained experimental results for three different mass flows in the thesis study. As the pressure loss increased with mass flow rate, it was concluded that lip separation had a detrimental effect on aerodynamic interface distortion. Additionally, different turbulence models were used in simulation results and compared with each other. The Reynolds Stress Model yielded the best results. It was concluded that simulation results supported the experimental data.

Nguyen [16] also concluded that flow separation and vortex formation occur inside the S-duct. Pressure loss increased with increasing Mach number, leading to pressure distortions at the engine inlet. The effects of vortices and secondary flows on flow distortion were investigated.

Chiang et al. [17] make the aerodynamic shape optimization of a boundary-layer-ingesting S-duct inlet for subsonic UAVs with embedded engines. By reshaping the duct walls, distortion was reduced and pressure recovery was increased.

To achieve better aerodynamic performance in S-ducts, this study investigated the effects of different jet intensities on flow separation. Additionally, the mechanism of pulsating jets in controlling separation was analyzed through flow separation characteristics within the S-duct. It has been observed that radial and axial pressure gradients in S-ducts play a critical role in the formation of secondary flows, and the pulse jet is an effective control method in weakening the flow separation. It has also been concluded that the pulse jet significantly reduces the vortex core loss and, accordingly, increases the dispersion effect in the flow [18].

Wang et al. [19] investigated the effects of co-rotating vortex generators on the flow field in a curved duct transitioning from elliptical to circular cross-section. Vortex generators placed on the lower surface of the first bend slightly reduced separation length and interacted more with the upper surface of the second bend, thereby modifying the internal pressure field and improving flow uniformity. Vortex generators placed only on the upper surface of the second bend did not significantly change flow uniformity. Installing vortex generators on both the lower surface of the first bend and the upper surface of the second bend improved overall flow uniformity, except



at the upper region of the engine interface plane. Numerical simulations were performed to investigate the impact of vortex generator placement. The study considered a baseline configuration without vortex generators and four different layout scenarios. Placing vortex generators only on the second bend resulted in lower flow uniformity with a DC60 value of 24.12. Placing them only on the first bend yielded better flow uniformity with a DC60 value of 20.7. Installing vortex generators on both bends provided the best flow uniformity with a DC60 of 18.7. However, the configuration with vortex generators on both bends significantly increased the total pressure loss. Considering the trade-off between DC60 and total pressure recovery, placing vortex generators only on the first bend is more advantageous, as it provides a slightly better pressure recovery with a DC60 of 20.7 compared to the both-bends configuration.

Tanguy et al. [20] used two different S-duct configurations and experimentally measured the total pressure losses and distortion levels. Inlets with higher curvature angles exhibited more severe total pressure distortions.

Bae et al. [21] validated the Efficient Global Method with various test functions. When applied to S-duct shape design with two different design variables, a global minimum was searched across the design space after three samplings. The results showed that this method is effective in identifying globally optimal solutions for complex 3D internal flow design problems.

Tanguy et al. [22] presented the effects of flow controllers (especially vortex generators) on the time-dependent flow field at the inlet and outlet of S-ducts. It was found that total pressure loss was associated with two counter-rotating vortices, and adding a flow controller significantly reduced the DC60 parameter with reductions up to 50% observed in some configurations. Pressure recovery increased in all cases. Moreover, increasing the angular placement of circumferential flow controllers stabilized the flow.

D'ambros et al. [23] investigated a numerical method to reduce flow distortions and pressure losses inside an S-duct. Vortices and pressure losses were identified as the main causes, and the aim was to reduce them. The optimization yielded approximately a 14% reduction in pressure loss and about a 71% reduction in vortex strength. A rectangular cross-section yielded the best result in terms of pressure loss, while a triangular section was optimal for vortex reduction.

Furlan et al. [24] optimized the upper and lower surface curvatures of a rectangular S-duct to minimize pressure loss and outlet distortion after selecting the appropriate turbulence model and mesh configuration. Fixed duct length and offset constraints were used in the optimization. The findings demonstrated that the method could be used for air intake design of engines with distributed propulsion systems.

Bhat et al. [25] compared different turbulence models available in Fluent 13.0. The performance of offset and expanding ducts was evaluated, and the behavior of turbulence models in flow control situations using the Zero Net Mass Flux technique was examined. It was observed that the SST  $k-\omega$  turbulence model yielded the best results.

Lee et al. [26] performed CFD analysis of RAE M 2129 S-duct and investigated the effect of inlet geometry aspect ratio. The SST  $k-\omega$  turbulence model was used, and the performance of the S-duct was evaluated using the distortion coefficient. The computational results were compared with experimental data. It was found that the semi-circular cross-section yielded the best results in all tested scenarios.

Zeng et al. [27] developed a fast and multi-objective optimization method for S-duct designs with bucket-type inlets and outlets. The SST  $k-\omega$  turbulence model was used, and a simplified and efficient method was developed to reduce computational costs in the optimization system. Compared to the original inlet, the optimized inlet achieved an increase in pressure recovery from 97% to 97.4%, and the DC60 parameter decreased by 21.7% at the design Mach number. The optimization objectives in this study were DC60 and total pressure recovery.



Rider et al. [28] selected an S-duct operating at Mach 0.8. The SST k- $\omega$  turbulence model was used and proved more successful in predicting separation points compared to previous attempts. The tubercle geometry in the flow control duct was successful in reducing or eliminating separation in the representative S-duct under transonic flow conditions.

The aim of this study is to investigate the aerodynamic performance of S-duct geometries and to evaluate critical performance parameters such as pressure recovery and flow distortion. In this context, a baseline S-duct design was developed and CFD simulations were conducted to analyze the flow behavior in detail. The results obtained provide valuable insights for designing more efficient and low-distortion inlet systems. In this context, this study includes the flow analyses of the S-duct, which is primarily used in combat aircrafts and also designed for UAVs. It examines two different geometric shapes under varying flight conditions, differing from previous studies and existing S-duct designs. The analyses are conducted based on the flight conditions in which UAVs can operate. Since it is known that values such as static pressure, turbulence and kinetic energy directly affect flight performance, the analysis and calculation of such values are of critical importance for flight performance. Therefore, this study will provide insight into the performance assessment of the S-duct geometry for use in aircrafts.

## 2. Material and Methods

The methodology for aerodynamic evaluation of the S-duct can be divided into five main components including geometry parameterization, mesh deformation, flow solver, gradient computation, and the Mach number. The Mach number is the parameter that needs to be determined to start the design and calculate the inlet area, which was taken as 0.3 M for the analysis. The Mach number considered in this study is a value at which UAVs can fly. With this consideration, the required velocity calculation was performed for 6000 meters, where the analysis was conducted, and it was found to be 94.93 m/s. Subsequently, considering previous studies, the mass flow rate was determined to be 0.281 kg/s using the interpolation method. As a result of these calculations, the inlet cross-sectional area was determined to be 4490 mm<sup>2</sup> using the continuity equation and the necessary parameters for the design were obtained. CFD parameters are given in Table 1.

**Table 1.** CFD parameters

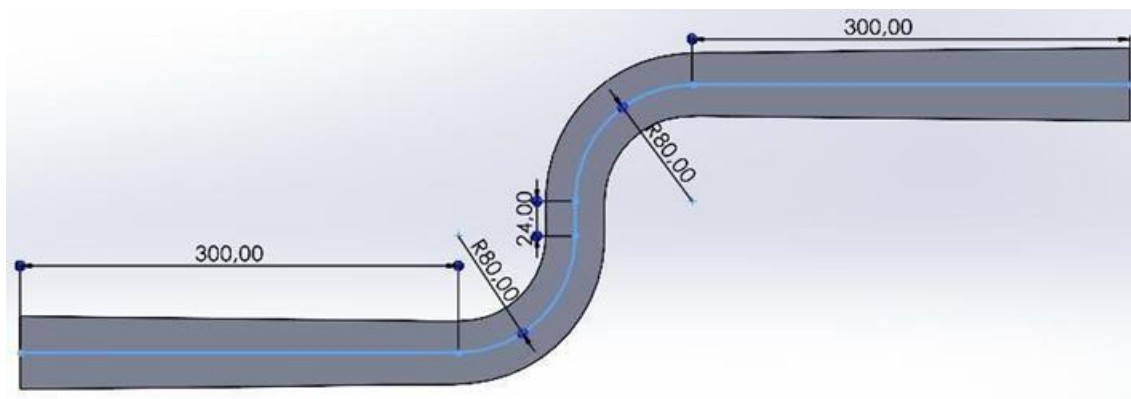
Parameter	Value
Velocity (m/s)	94.93
Altitude (m)	6000
Density (kg/m <sup>3</sup> )	0.66011
Mass flow rate (kg/s)	0.281
Area (m <sup>2</sup> )	0.004490
Turbulence model	SST k- $\omega$

In the design procedure, S-ducts with rectangular and circular cross sectional areas were modelled using SOLIDWORKS. All designs created for CFD analysis were then transferred to the ANSYS Fluent. To ensure a valid performance analysis for all geometries, the inlet and outlet sectional areas were kept the same. The turbulence model was chosen as the SST k- $\omega$  turbulence model based on literature. The model can make more accurate separation predictions compared to standard models [12].

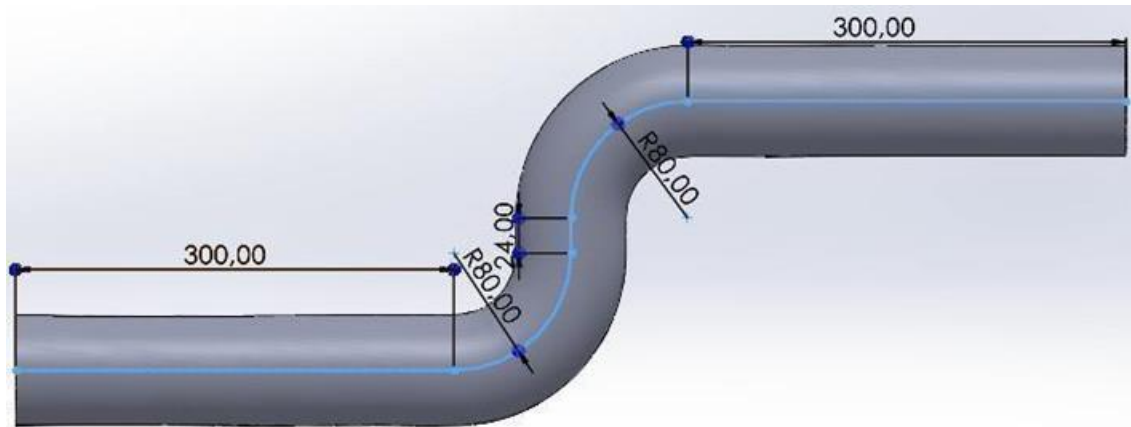
Since a narrowing structure in the throat section of the duct, relative to the capture area ( $A_c$ ), increases the flow rate and reduces static pressure, it is an important design consideration. The contraction ratio ( $CR = A_t/A_c$ ), which defines the relationship between the throat area ( $A_t$ ) and the capture area ( $A_c$ ), was set to 0.75 based on previous studies. The design was carried out accordingly [8].



Figure 1 and Figure 2 show the rectangular and circular S-duct designs where the inlet and outlet areas are kept the same and the duct has a narrowing structure. The bends in the duct have a radius of 80 mm, and the dimension that the flow will follow until it turns and exits the turn is 300 mm. The rectangular S-duct has a width of 89.5 mm and a length of 50.167 mm. The width and length of the S-duct are very important. These dimensions directly affect the character of the air flow passing through it. Width and length play a decisive role in factors such as pressure losses, flow separation, turbulence formation and smoothness of flow at the engine inlet. An improperly designed duct can lead to loss of efficiency, reduced engine performance and even aerodynamic imbalances. Therefore, both width and length should be optimized for aerodynamic performance.



**Figure 1.** Rectangular S-duct design



**Figure 2.** Circular S-duct design

Figures 3, 4, 5, 6, 7 and 8 show the mesh network applied to the considered S-duct geometries. After the design was completed, the analyses were performed. For circular and rectangular sections, the mesh size was 5 mm, edge sizing was given to the inlet and outlet parts of the geometries, and then the mesh network was created using the inflation command.

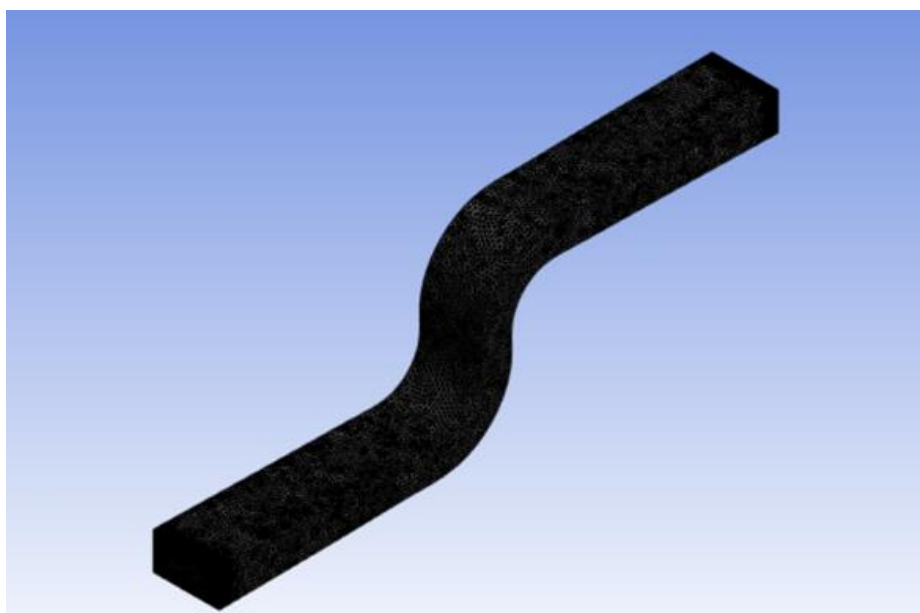


**Figure 3.** Rectangular S-duct meshing

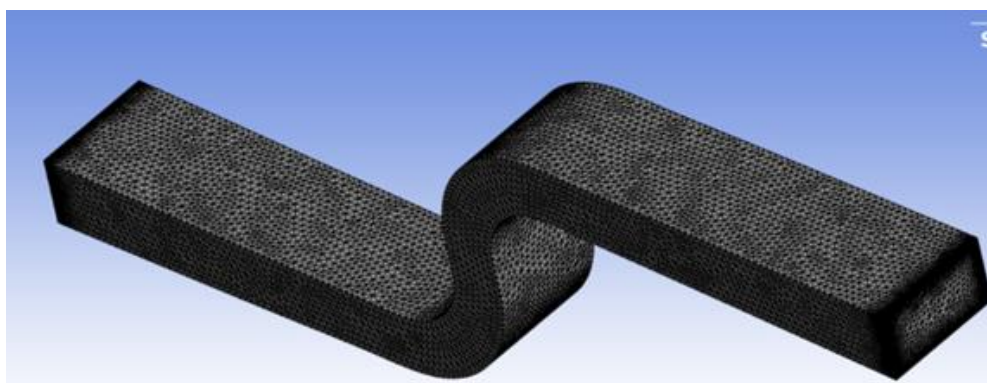


**Figure 4.** Rectangular S-duct meshing

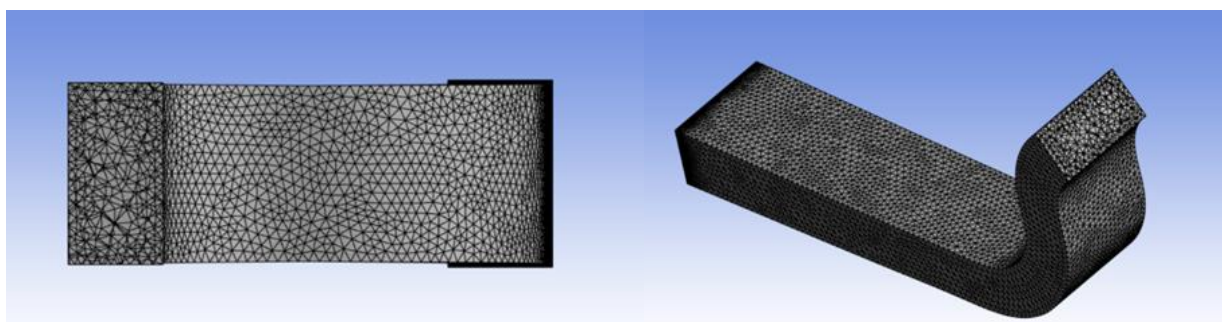


**Figure 5.** Rectangular S-duct meshing section views

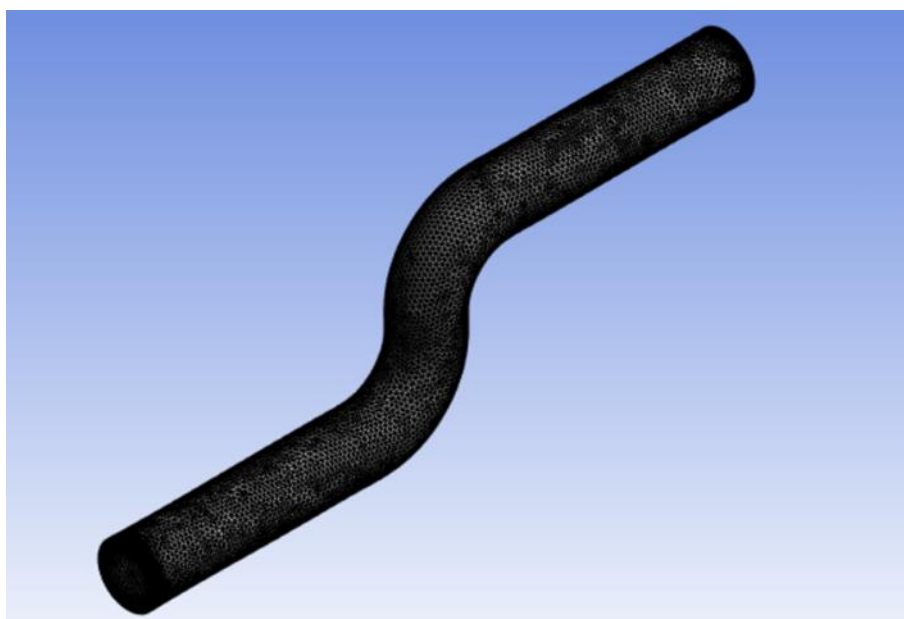


**Figure 6.** Circular S-duct meshing

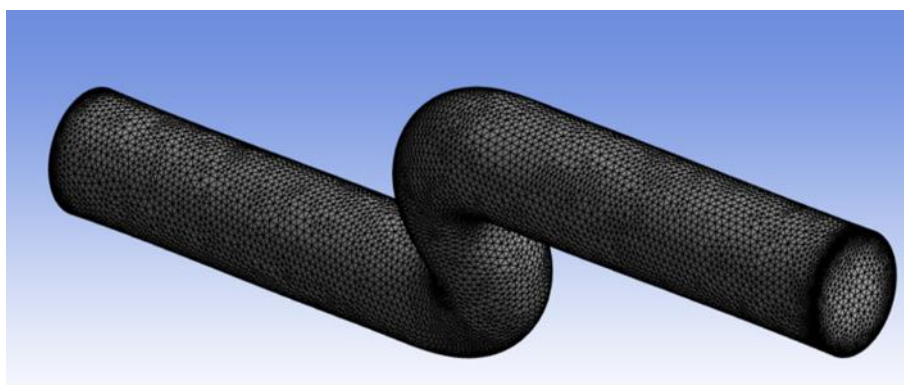


**Figure 7.** Circular S-duct meshing

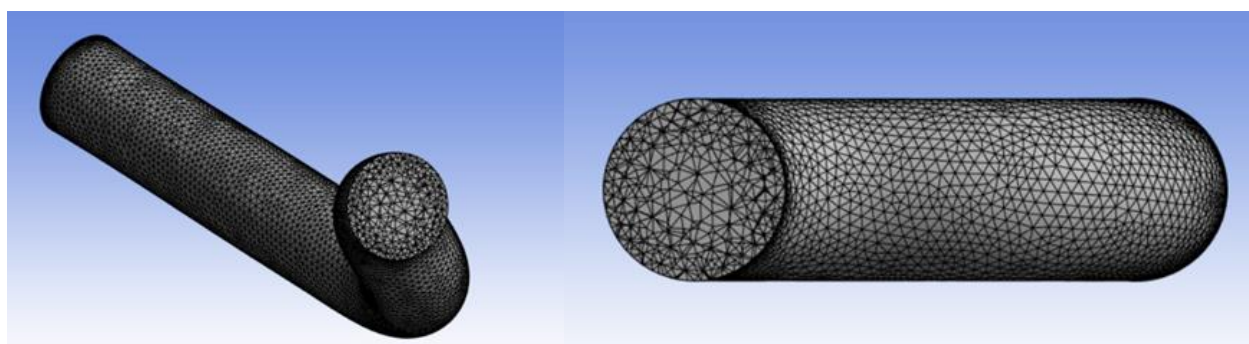


**Figure 8.** Circular S-duct meshing section views

The critical parameters obtained for the rectangular and circular S-ducts as a result of the mesh convergence examination are presented in Table 2 and 3, respectively.



**Table 2.** Mesh convergence for rectangular S-duct

Mesh size (mm)	Distortion Coefficient (DC60)	Pressure Recovery (PR)
7	0.06946	0.6931
6	0.06893	0.6983
5	0.06875	0.6986

**Table 3.** Mesh convergence for circular S-duct

Mesh size (mm)	Distortion Coefficient (DC60)	Pressure Recovery (PR)
7	0.06299	0.7559
6	0.06297	0.7565
5	0.06286	0.7589

The number of elements, skewness ratio and orthogonal quality for each geometry are provided in Table 4. Mesh quality is assessed by orthogonal quality and skewness values. When the results obtained above are compared with the mesh metric visual provided in Figure 9, which shows that the mesh quality is within the appropriate intervals.

**Table 4.** Mesh metrics

Duct Geometry/Mesh Parameter	Rectangular Duct	Circular Duct
Number of Elements	261367	197413
Skewness	Max: 0.79823	Max: 0.7954
	Min: 8.8669e-005	Min: 5.9588e-004
	Average: 0.22668	Average: 0.22583
	Max: 0.99685	Max: 0.2046
Orthogonal Quality	Min: 0.20177	Min: 0.11662
	Average: 0.77204	Average: 0.77287

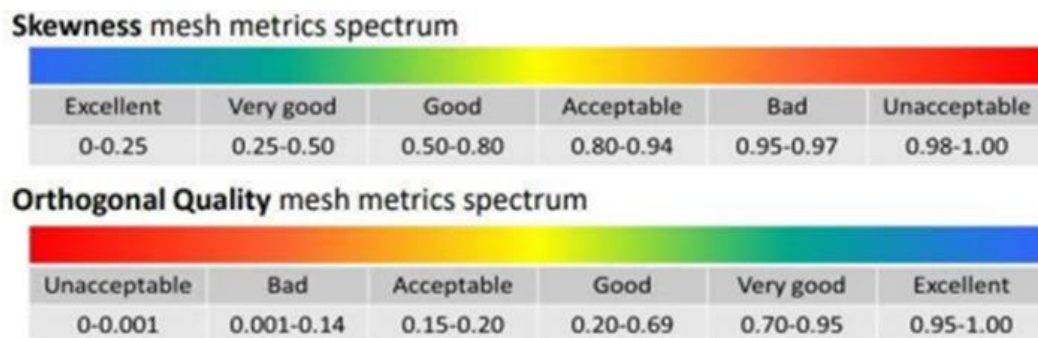


**Figure 9.** Mesh metrics spectrum [14]

### 3. Results

In this section, static pressure, velocity and turbulence kinetic energy contours are given for circular and rectangular ducts, respectively, and are interpreted separately.

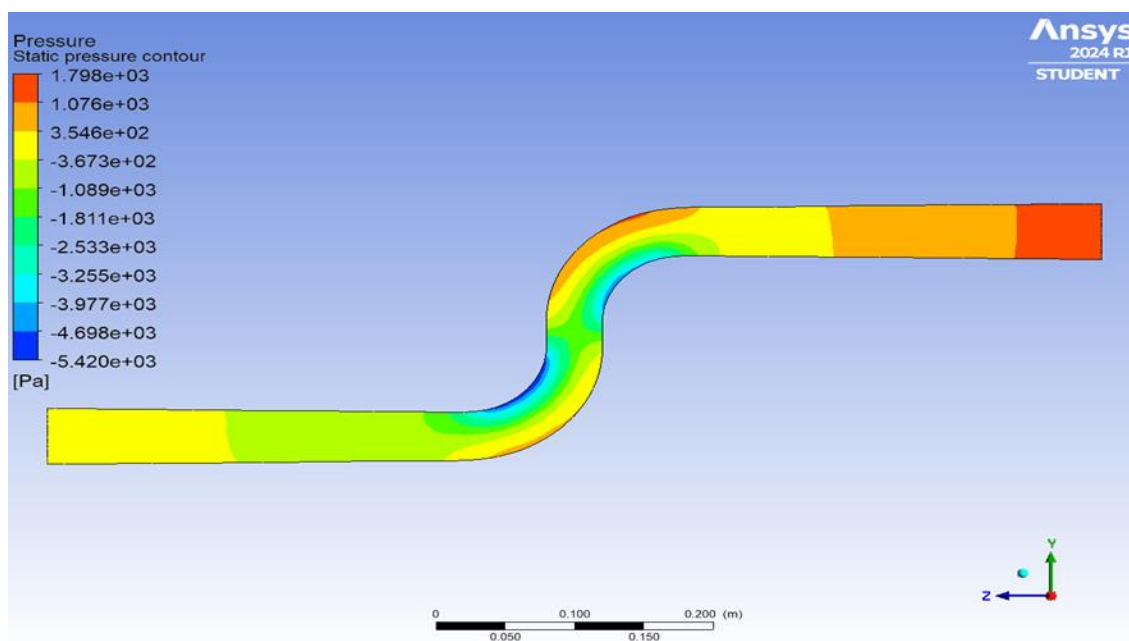


Figure 10. Rectangular S-duct static pressure contour

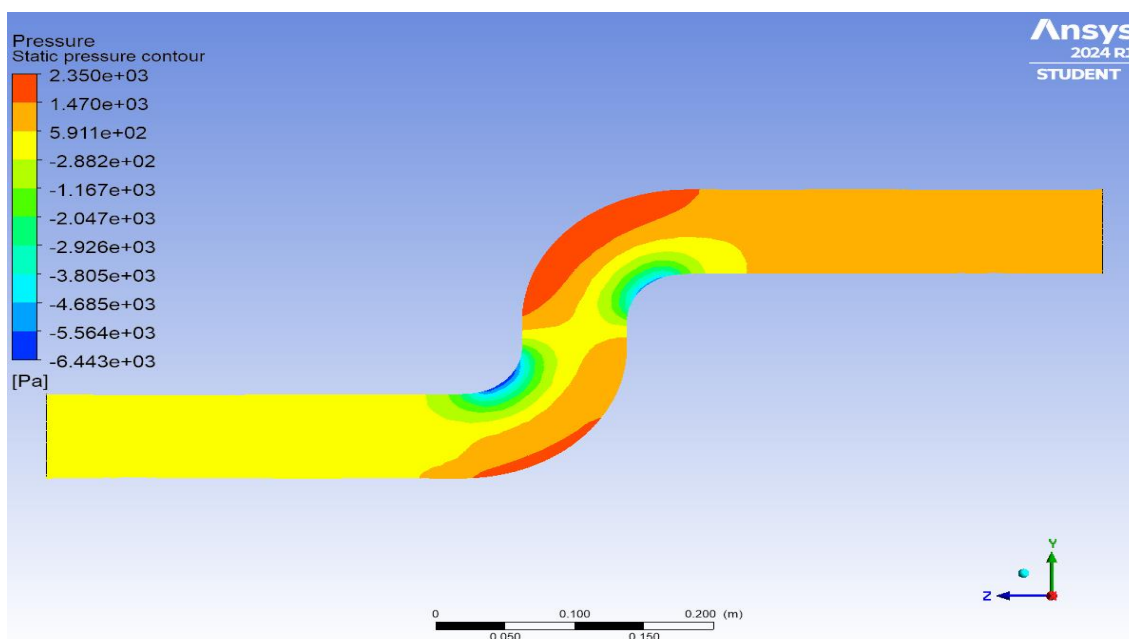
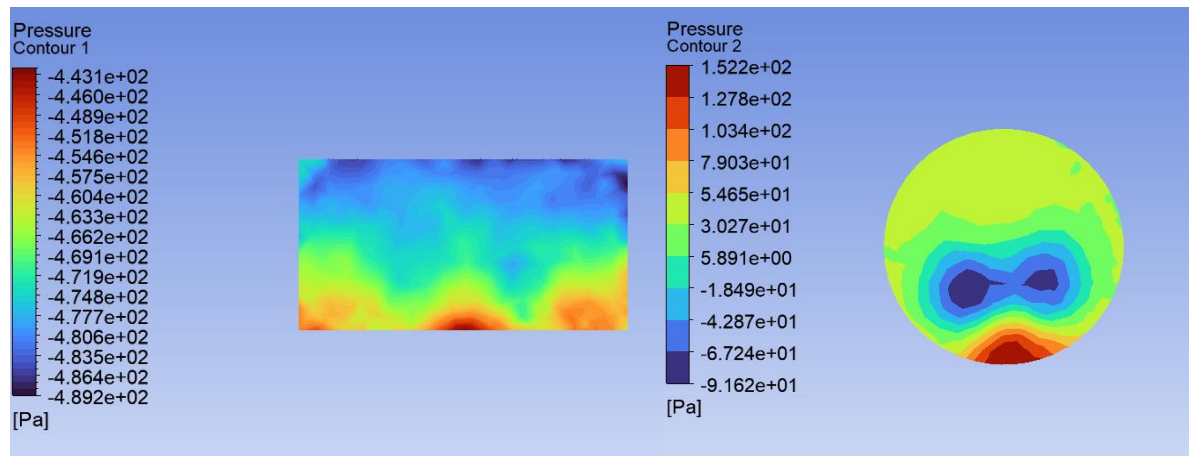
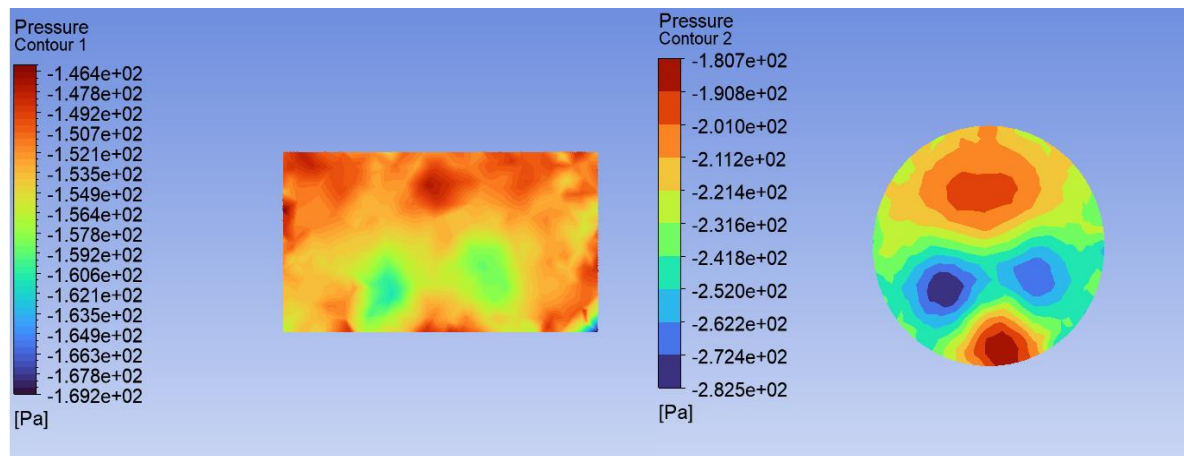


Figure 11. Circular S-duct static pressure contour



**Figure 12.** The pressure distribution for both S-ducts at a distance of 160 millimeters downstream of the duct exit



**Figure 13.** The pressure distribution for both S-ducts at a distance of 60 millimeters downstream of the duct exit

Energy consumption and stress on the system increase with high static pressure. Increased stress can damage the duct and the structures connected to the duct. At the same time, it is possible to say that the irregularities and turbulence in the flow increase at high stress values according to the distribution on the duct geometry. These irregularities and turbulence in the flow create a negative effect aerodynamically during the flight time. It is shown in Figure 10 and 11 that the maximum static pressure on the circular S-duct was found to be  $2.350 \times 10^3$  Pa, while the maximum static pressure on the rectangular S-duct was  $1.798 \times 10^3$  Pa. The pressure distributions for both S-ducts at distances of 60 millimeters and 160 millimeters downstream of the duct exit are shown in Figure 12 and 13. As a result of this analysis, the static pressure distribution of the rectangular duct is more efficient than the circular duct and the maximum static pressure value is much lower which is preferable.

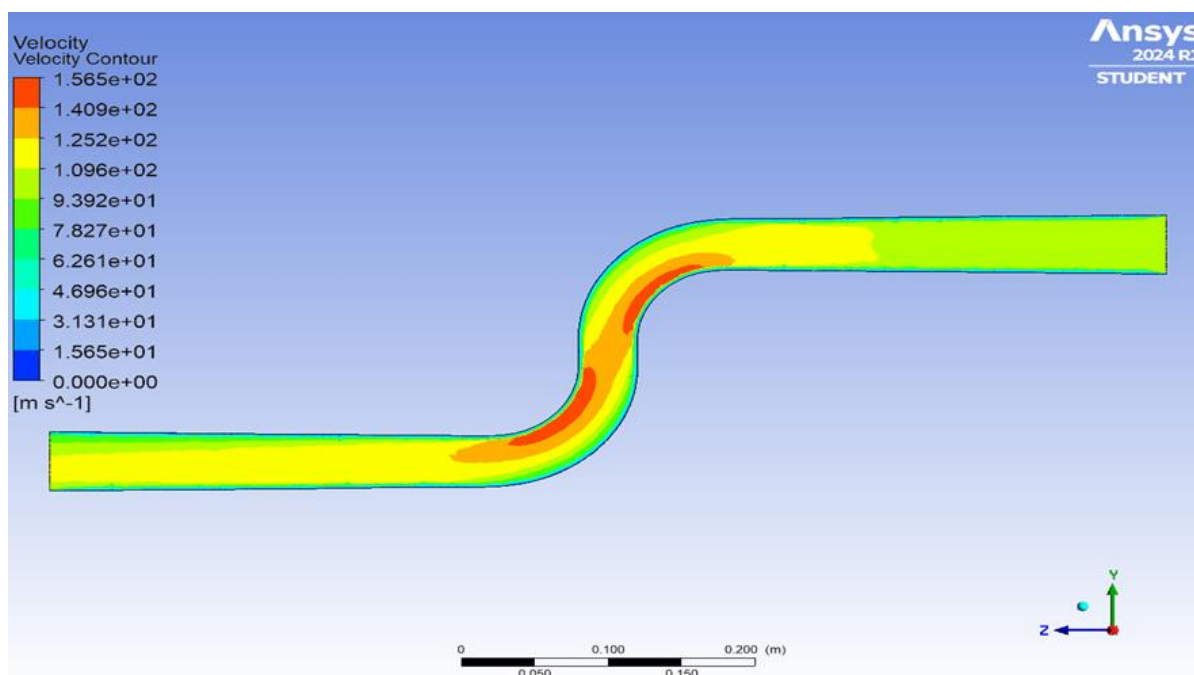


Figure 14. Rectangular S-duct velocity contour

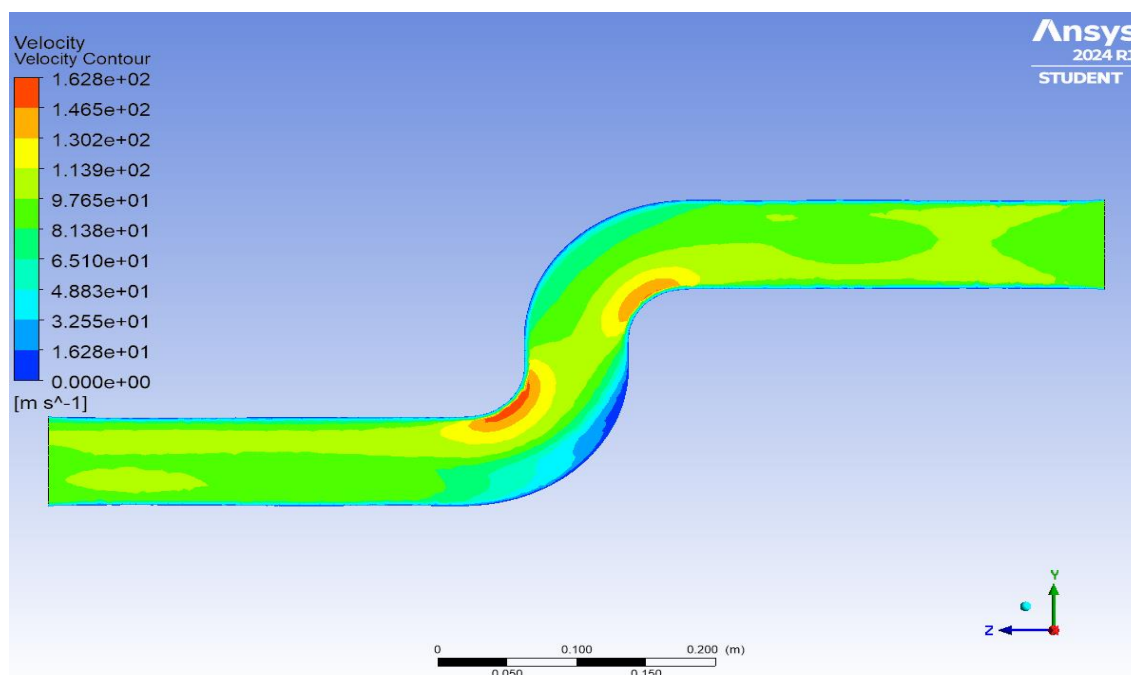
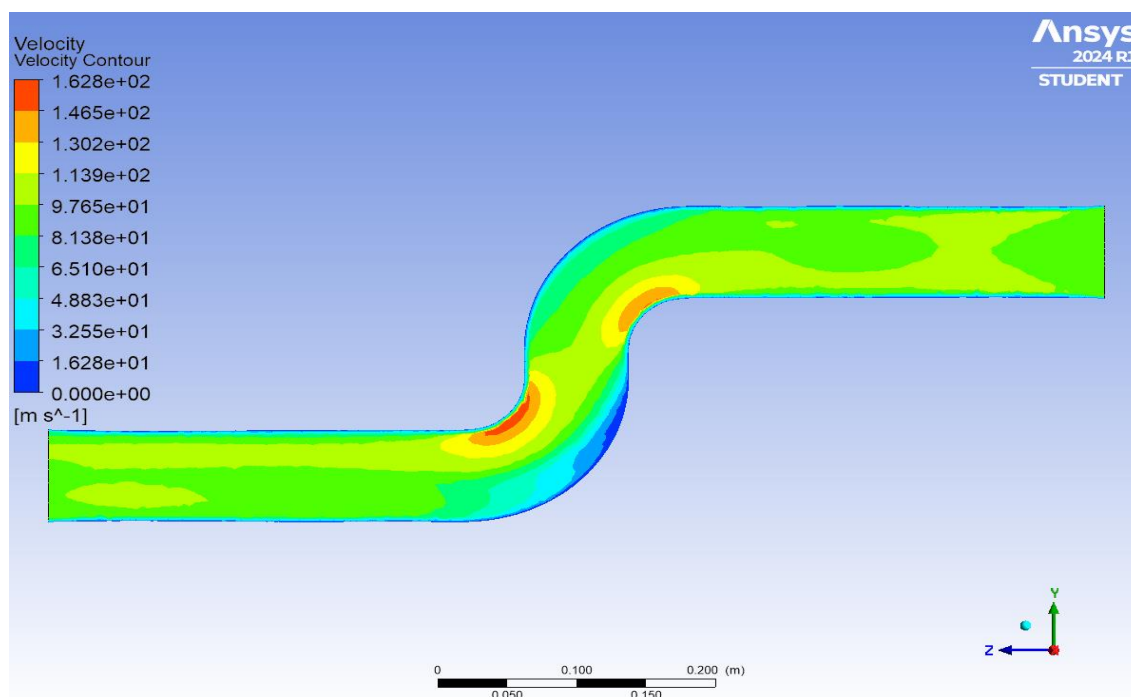
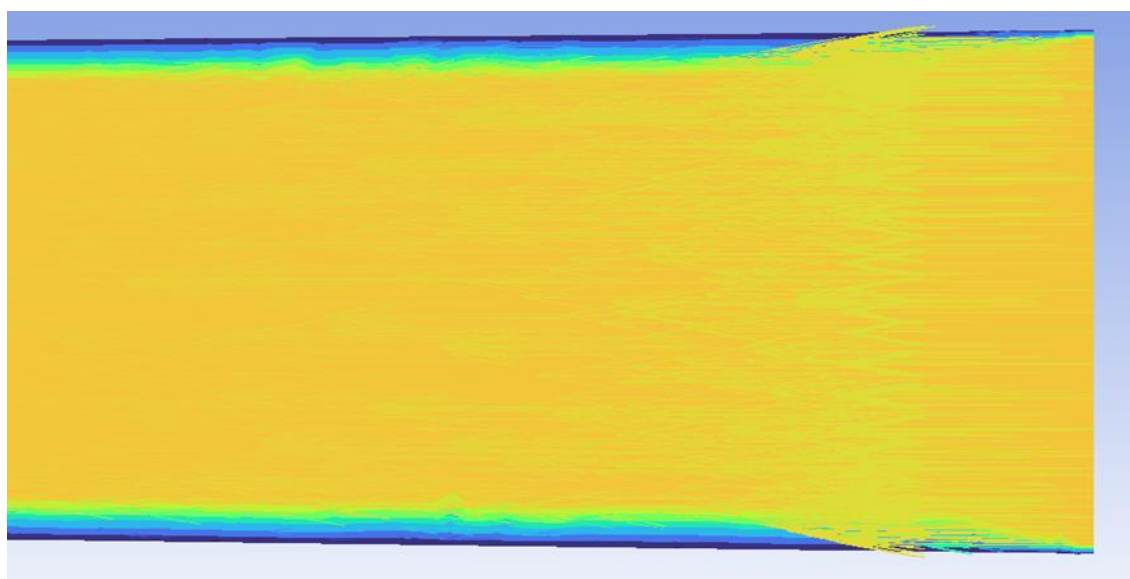


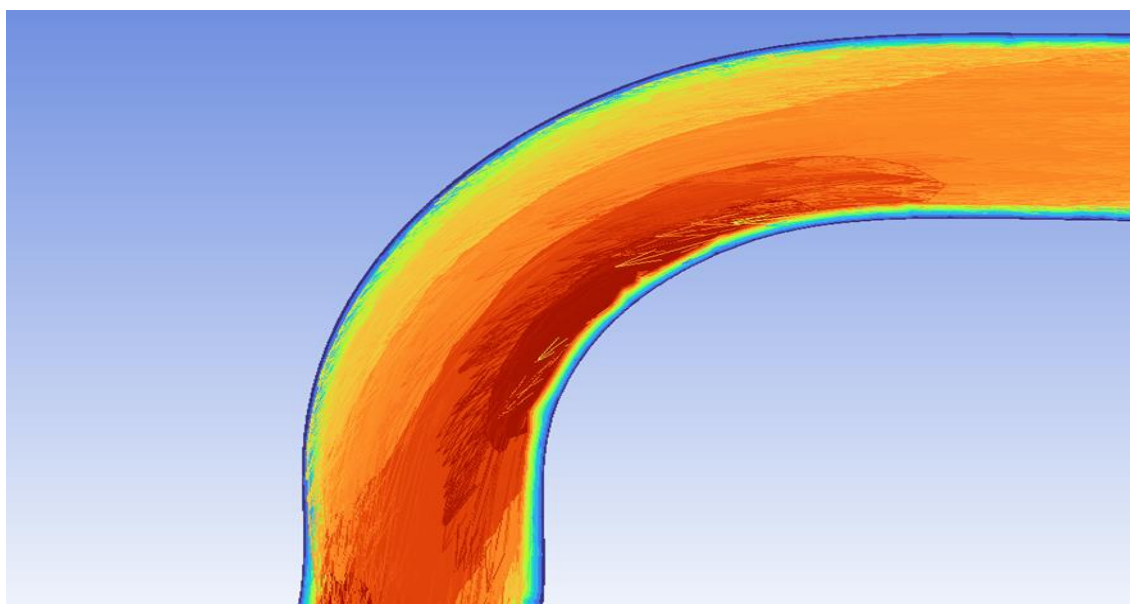
Figure 15. Circular S-duct velocity contour



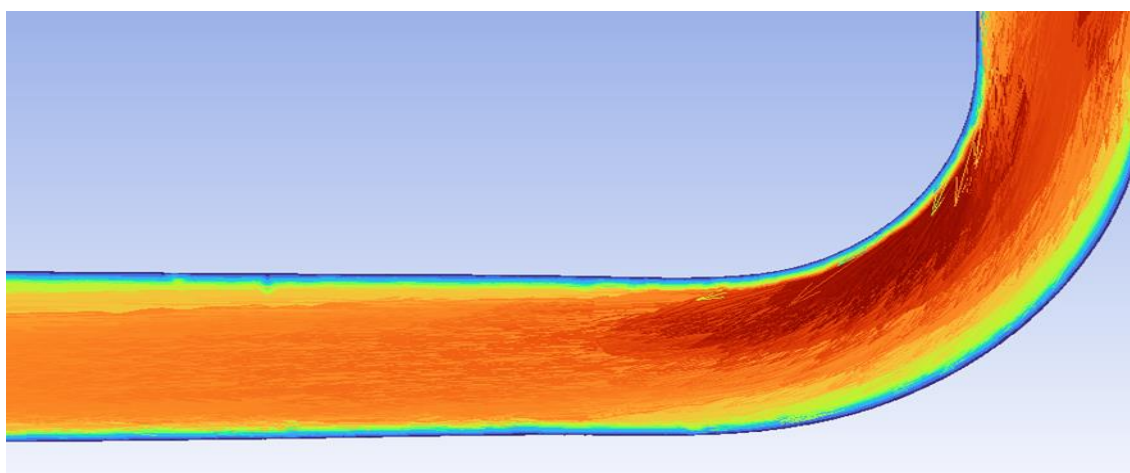
**Figure 15.** Circular S-duct velocity contour



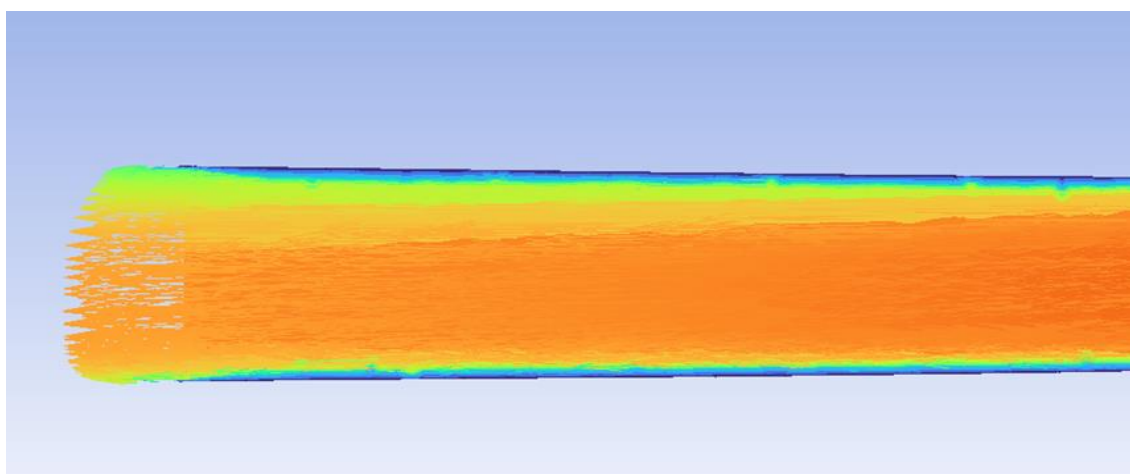
**Figure 16.** Detailed velocity contour and vector inlet view of the rectangular S-duct



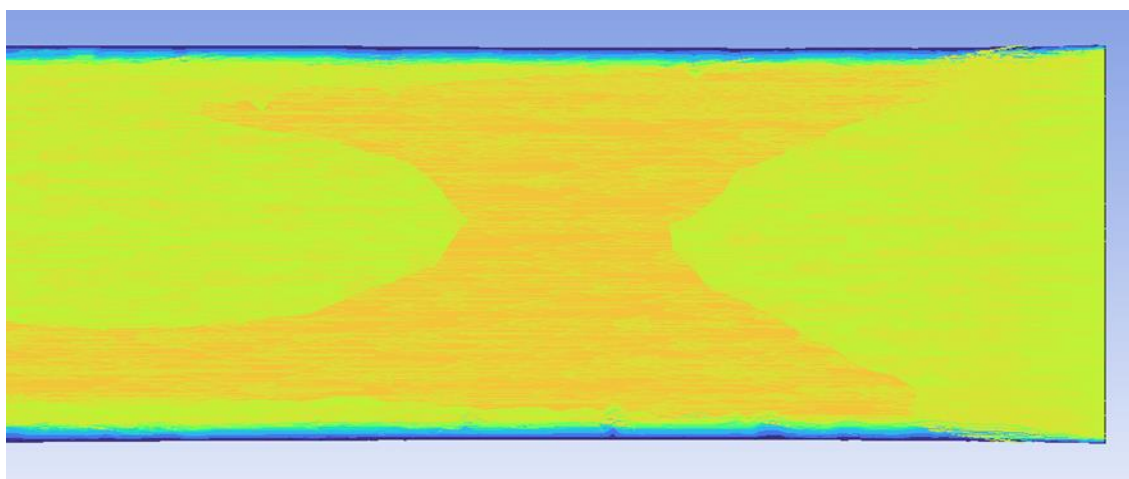
**Figure 17.** Detailed velocity contour and vector first curve view of the rectangular S-duct



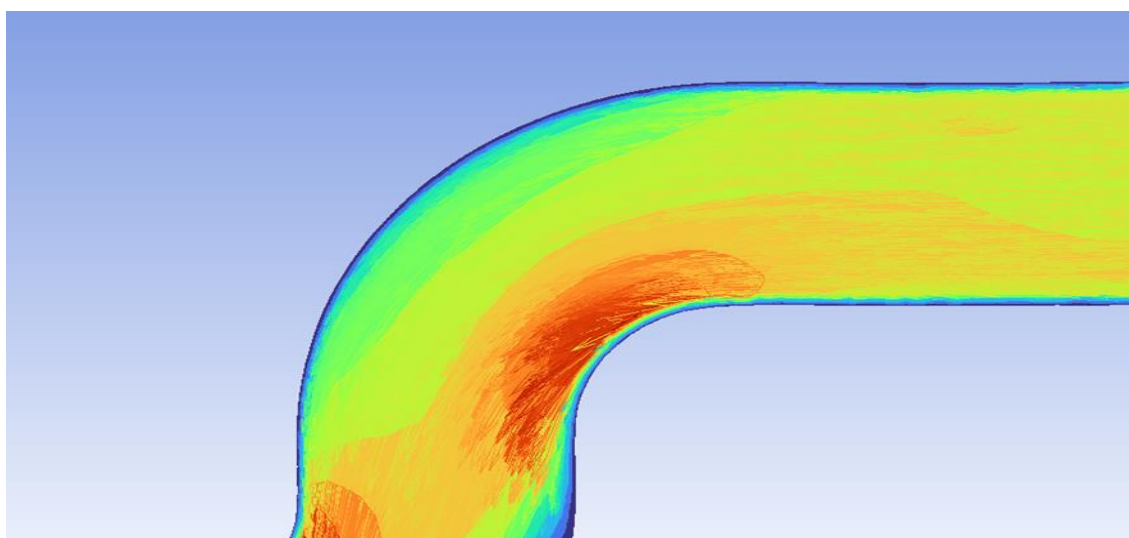
**Figure 18.** Detailed velocity contour and vector second curve view of the rectangular S-duct



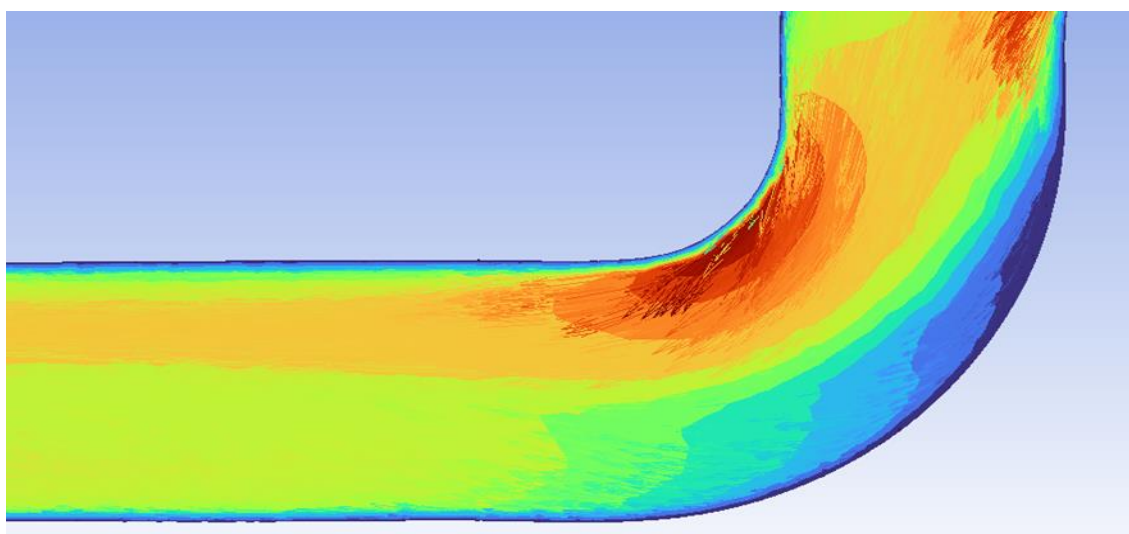
**Figure 19.** Detailed velocity contour and vector outlet view of the rectangular S-duct



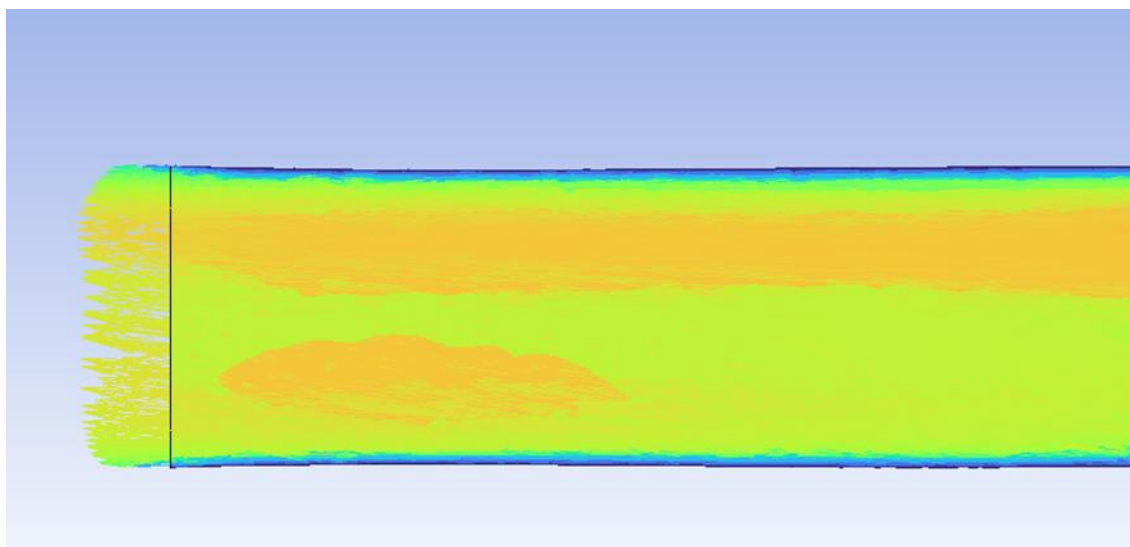
**Figure 20.** Detailed velocity contour and vector inlet view of the circular S-duct



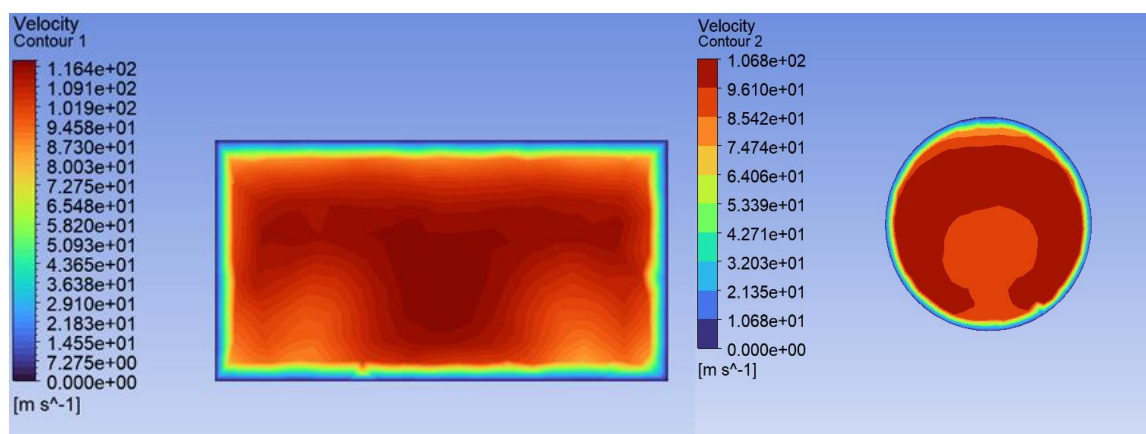
**Figure 21.** Detailed velocity contour and vector first curve view of the circular S-duct



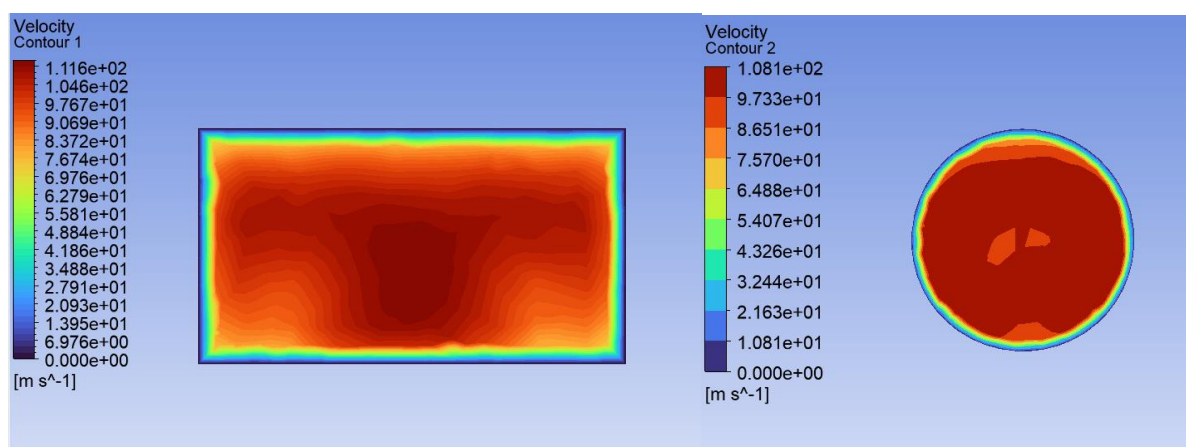
**Figure 22.** Detailed velocity contour and vector second curve view of the circular S-duct



**Figure 23.** Detailed velocity contour and vector outlet view of the circular S-duct



**Figure 24.** The velocity distribution for both S-ducts at a distance of 160 millimeters downstream of the duct exit



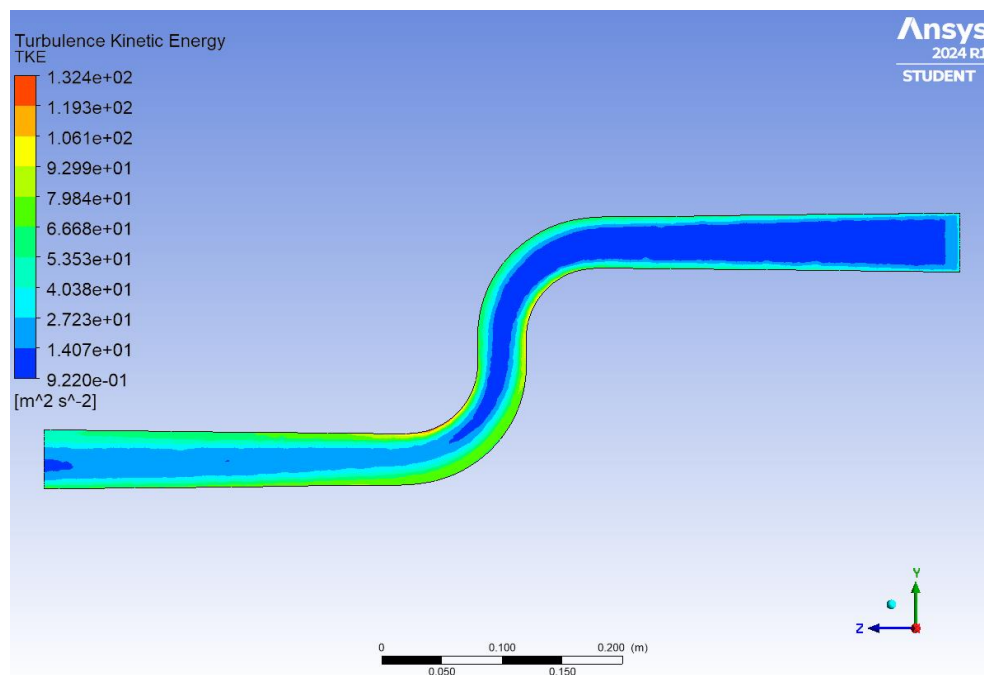
**Figure 25.** The velocity distribution for both S-ducts at a distance of 60 millimeters downstream of the duct exit



Figure 14 and 15 show that the maximum airflow velocity inside the circular S-duct was  $1.628\text{e}+02$  m/s, while the maximum velocity value was obtained as  $1.565\text{e}+02$  m/s inside the rectangular S-duct. In the rectangular S-duct, the wall effect is high and the boundary layer thickness increases at the corners, which creates additional friction in the flow. This explains why the velocity in the rectangular S-duct is lower than that in the circular S-duct.

Comparing the corresponding pressure contours in Figure 10 and 11, and airflow velocity contours in Figure 14 and 15 reveal that pressure decreases in areas where velocity increases and velocity increases in areas where pressure decreases.

The detailed velocity contour and velocity vectors are shown in Figure 16 to 23. Also, velocity distributions for both S-ducts at a distance of 60 millimeters and 160 millimeters downstream of the duct exit are shown in Figure 24 and Figure 25. For both S-ducts, there was an increase in velocity in the concave regions. For circular S-ducts, in Figure 24 and Figure 25 the flow appears mostly homogeneous; although there are slightly lower velocities at the center, overall circular symmetry is maintained. The two small low-velocity regions at the center may indicate the presence of secondary flow effects. A distinct low-velocity region has formed at the center, which may indicate that the flow has shifted outward from the center. Such a profile is typically associated with flow separation and the intensification of secondary flows. S-ducts that have two non-planar bends may increase pressure gradients. Especially in the concave surfaces, the flow was directed toward the walls due to centrifugal effects. This results in lower velocities at the center and higher velocities near the outer edges. The vortex pairs developing within the duct may cause the flow to be directed toward specific regions. This becomes more pronounced toward the outlet and results in low-velocity regions at the center and high-velocity rings near the edges. The velocity profile observed for the rectangular S-duct is a conventional velocity profile (see Figure 24 and 25).



**Figure 26.** Rectangular S-duct turbulent kinetic energy contour

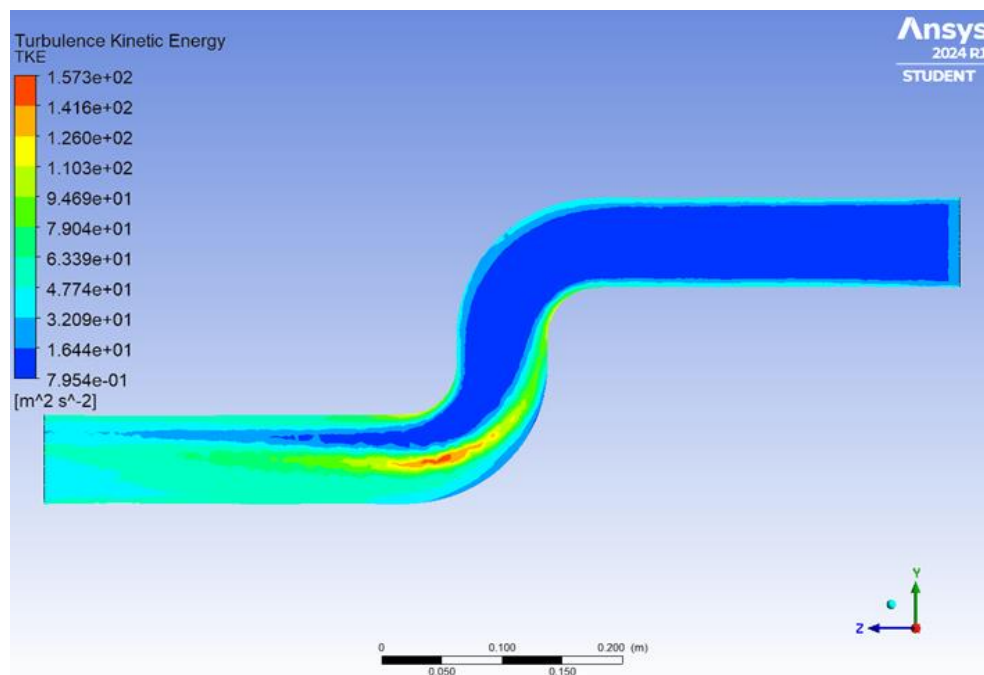


**Figure 27.** Circular S-duct turbulent kinetic energy contour

Relatively low turbulent kinetic energy reduces the energy loss and drag force in the system. As the drag force in the system decreases, flight becomes more efficient in terms of reduced fuel consumption. However, if relatively high turbulent kinetic energy is carried in turbulent flows, it is likely that the turbulent kinetic energy distribution becomes crucial in the components used for propulsion system applications such as S-duct. Figure 26 and 27 show that the maximum turbulent kinetic energy value in the circular S-duct was around  $1.573 \times 10^2 \text{ m}^2/\text{s}^2$ , while the maximum turbulent kinetic energy value in the rectangular S-duct was attained as  $1.324 \times 10^2 \text{ m}^2/\text{s}^2$ . This analysis proved that the turbulent kinetic energy distribution of the rectangular duct seems to be more efficient than the circular duct.

Table 5 briefly summarizes the overall CFD results. It can be stated that the maximum static pressure of the rectangular S-duct is lower and better distributed than the circular S-duct. The maximum value of the turbulent kinetic energy is lower in the rectangular S-duct than in the circular S-duct. It was also observed that the distribution of turbulent kinetic energy is uniform for the rectangular S-duct.

**Table 5.** CFD analysis results

Duct Geometry/Analysis Result	Rectangular Duct	Circular Duct
Static Pressure (Pa)	Max: $1.798 \times 10^3$	Max: $2.350 \times 10^3$
	Min: $-5.420 \times 10^3$	Min: $-6.443 \times 10^3$
Velocity (m/s)	Max: $1.585 \times 10^2$	Max: $1.628 \times 10^2$
	Min: 0	Min: 0
Turbulent Kinetic Energy ( $\text{m}^2/\text{s}^2$ )	Max: $1.324 \times 10^2$	Max: $1.573 \times 10^2$
	Min: $9.220 \times 10^{-1}$	Min: $7.954 \times 10^{-1}$



#### 4. Conclusion

In this study, the aerodynamic performance of circular and rectangular S-ducts is investigated under the specified flight conditions. Two different models were designed in SOLIDWORKS to analyze certain parameters, including static pressure, airflow velocity, and turbulent kinetic energy, using ANSYS Fluent.

As a result of the series of analyses, the concluding remarks can be outlined as follows;

- The rectangular S-duct performs better in terms of static pressure compared to the circular S-duct. A decrease in static pressure reduces energy consumption and system stress, thereby improving overall efficiency.
- On the other hand, increased, non-uniform static pressure and turbulent kinetic energy increase vibration and noise in the system.
- Although the pressure and velocity distribution is more uniform in the rectangular S-duct, the circular S-duct performs better compared to the rectangular S-duct in terms of pressure recovery and distortion coefficient.
- The velocity profile observed in the circular S-duct may be caused by factors such as geometric curvatures, pressure gradients and wall effects, vortex formation, and secondary flows.

#### Future Research

Within the scope of this study, basic geometries were considered and analyses were performed. In the continuation of the study, different optimized geometries used in practice will also be analyzed. Moreover, the numerical analysis results, in this article, could not be verified due to lack of experimental data. As the authors cannot validate it with experimental data, in order to ensure the reliability of the results, the numerical analysis results will be validated by experimental study results in future studies.

#### Acknowledgment

*This article was developed by expanding and partially modifying the content of the paper entitled 'Comparative Analysis of Circular and Rectangular S-Ducts: Optimising Aerodynamic Performance and Flow Efficiency using CFD Modelling,' which was presented orally at the ICAA'24 International Conference of Aeronautics and Astronautics Symposium; however, the full-text was not published.*

#### Authorship contribution statement

**Mehmet Turan Ekinci**, Conceptualization, Software, Data curation, Writing – original draft. **Mahmut Sami Bükür**, Conceptualization, Writing – review & editing, Supervision.

**Conflicts of Interest:** The author declares no conflict of interest.

#### References

- [1] Aref, P., Ghoreyshi, M., Jirasek, A. and Satchell, M. J. 2018. CFD validation and flow control of RAE-M2129 S-Duct diffuser using CREATETM-AV kestrel simulation tools. *Aerospace*, 5(1), 31.
- [2] Meneghin, A. 2020. "Three-objective optimization studies of an S-duct". M.Sc. thesis, Università degli Studi di Padova, Dipartimento di Ingegneria Industriale, Padova, Italy, 1-122.
- [3] Thenambika, V., Ponsankar, S., and Prabhu, M. K. 2016. Design and flow analysis of S duct diffuser with submerged vortex Generators. *International Journal of Engineering Research and Applications*, 6(2), 79-84.



- [4] Immonen, E. 2018. Shape optimization of annular S-ducts by CFD and high-order polynomial response surfaces. *Engineering Computations*, 35(2), 932-954.
- [5] Rk, A. 2021. CFD Investigation on the Circular Rectangular and Ellipse shape on the Aerodynamics in S-Duct. *International Research Journal of Engineering and Technology (IRJET)*, 08(04), 2051-2059.
- [6] Lee, J., and Cho, J. 2018. Effect of aspect ratio of elliptical inlet shape on performance of subsonic diffusing S-duct. *Journal of Mechanical Science and Technology*, 32, 1153-1160.
- [7] Jiang, F., Kontis, K., and White, C. 2024. Numerical investigation and mode analysis of the S-duct. *Physics of Fluids*, 36(11), 115150.
- [8] Papadopoulos, F., Valakos, I., and Nikolos, I. K. 2012. Design of an S-duct intake for UAV applications. *Aircraft Engineering and Aerospace Technology*, 84(6), 439-456.
- [9] Saha, K., Singh, S. N., Seshadri, V., and Mukhopadhyay, S. 2007. Computational analysis on flow through transition S-diffusers: Effect of inlet shape. *Journal of aircraft*, 44(1), 187-193.
- [10] Migliorini, M., Zachos, P. K., MacManus, D. G., and Haladuda, P. 2023. S-duct flow distortion with non-uniform inlet conditions. *Proceedings of the Institution of Mechanical Engineers, Part G: Journal of Aerospace Engineering*, 237(2), 357-373.
- [11] Xiao, Q., Tsai, H. M., and Liu, F. 2003. Computation of Transonic Diffuser Flows by a Lagged k- $\epsilon$  Turbulence Model. *Journal of propulsion and power*, 19(3), 473-483.
- [12] Zhang, J. M., Wang, C. F., and Lum, K. Y. 2008. Multidisciplinary design of S-shaped intake. 26th AIAA Applied Aerodynamics Conference, 18-21 August, Honolulu, Hawaii.
- [13] McLelland, G., MacManus, D. G., Zachos, P. K., Gil-Prieto, D., and Migliorini, M. 2020. Influence of upstream total pressure profiles on S-duct intake flow distortion. *Journal of Propulsion and Power*, 36(3), 346-356.
- [14] Novia, P., Asngali, B., Susanto, A., Adzandy, R., and Purnomo, H. 2023. COMPUTATIONAL FLUID DYNAMIC (CFD) SIMULATION ON REDESIGN BAFFLES OF YOGYAKARTA INTERNATIONAL AIRPORT TRAIN FUEL TANK. *Media Mesin: Majalah Teknik Mesin*, 24(1), 1-24.
- [15] Aslan, S. 2017. "Experimental and Numerical Investigation of an S-Duct Diffuser Designed for a Micro Turbojet Engine Powered Aircraft ". M.Sc. thesis, Middle East Technical University, Graduate School of Natural and Applied Sciences, Ankara, Turkey.
- [16] Nguyen, S. 2013. "Computational fluid dynamics simulations of a diffusing S-duct using overset grids". Ph.D. thesis, California State University, Los Angeles, USA.
- [17] Chiang, C., Koo, D., and Zingg, D. W. 2022. Aerodynamic shape optimization of an S-duct intake for a boundary-layer ingesting engine. *Journal of Aircraft*, 59(3), 725-741.
- [18] Wang, C., Lu, H., Kong, X., Wang, S., Ren, D., and Huang, T. 2023. Effects of Pulsed Jet Intensities on the Performance of the S-Duct. *Aerospace*, 10(2), 184.
- [19] Shivakumar, B. B., Narahari, H. K., Jayasimha, P., and Sriram, A. T. 2023. Numerical study on the placement of vortex generator in a serpentine air intake duct. *Sādhanā*, 48(2), 81.
- [20] Tanguy, G., MacManus, D. G., Garnier, E., and Martin, P. G. 2018. Characteristics of unsteady total pressure distortion for a complex aero-engine intake duct. *Aerospace Science and Technology*, 78, 297-311.
- [21] Bae, H., Park, S., and Kwon, J. 2013. Efficient global optimization for S-duct diffuser shape design. *Proceedings of the Institution of Mechanical Engineers, Part G: Journal of Aerospace Engineering*, 227(9), 1516-1532.
- [22] Tanguy, G., MacManus, D. G., Zachos, P., Gil-Prieto, D., and Garnier, E. 2017. Passive flow control study in an S-duct using stereo particle image velocimetry. *AIAA journal*, 55(6), 1862-1877.



- [23] D’ambros, A., Kipouros, T., Zachos, P., Savill, M., and Benini, E. 2018. Computational design optimization for S-ducts. *Designs*, 2(4), 36.
- [24] Furlan, F., Chiereghin, N., Kipouros, T., Benini, E., and Savill, M. 2014. Computational design of S-Duct intakes for distributed propulsion. *Aircraft engineering and aerospace technology: an international journal*, 86(6), 473-477.
- [25] Bhat, S. P., and Sullerey, R. K. 2013. An assessment of turbulence models for S-duct diffusers with flow control. *Gas Turbine India Conference*, 5 December, 35161, Bangalore, Karnataka, India.
- [26] Lee, J., Choi, H., Ryu, M., and Cho, J. 2015. A Study on Flow Characteristics of the Inlet Shape for the S-Duct. *Journal of the Korean Society for Aeronautical & Space Sciences*, 43(2), 109-117.
- [27] Zeng, L., Pan, D., Ye, S., and Shao, X. 2019. A fast multiobjective optimization approach to S-duct scoop inlets design with both inflow and outflow. *Proceedings of the Institution of Mechanical Engineers, Part G: Journal of Aerospace Engineering*, 233(9), 3381-3394.
- [28] Rider, C. S. 2021. “Passive Flow Control in an S-duct Intake”. M.Sc. thesis, Royal Military College of Canada, Applied Science in Aeronautical Engineering, Ontario, Canada